Evidence for GN-z11 as a luminous galaxy at redshift 10.957

Linhua Jiang[1,2], Nobunari Kashikawa[3,4], Shu Wang[1,2], Gregory Walth[5], Luis C. Ho[1,2], Zheng Cai[6], Eiichi Egami[7], Xiaohui Fan[7], Kei Ito[3,8], Yongming Liang[3,8], Daniel Schaerer[9], and Daniel P. Stark[7]

[1]*Kavli Institute for Astronomy and Astrophysics, Peking University, Beijing, China*

[2]*Department of Astronomy, School of Physics, Peking University, Beijing, China*

[3]*Department of Astronomy, Graduate School of Science, The University of Tokyo, Tokyo, Japan*

[4]*Optical and Infrared Astronomy Division, National Astronomical Observatory, Tokyo, Japan*

[5]*Observatories of the Carnegie Institution for Science, Pasadena, CA, USA*

[6]*Department of Astronomy, Tsinghua University, Beijing, China*

[7]*Steward Observatory, University of Arizona, Tucson, AZ, USA*

[8]*Department Astronomical Science, SOKENDAI (The Graduate University for Advanced Studies), Tokyo, Japan*

[9]*Geneva Observatory, University of Geneva, Geneva, Switzerland*

GN-z11 was photometrically selected as a luminous star-forming galaxy candidate at redshift $z > 10$ based on Hubble Space Telescope (HST) imaging data[1]. Follow-up HST near-infrared grism observations detected a continuum break that was explained as the Lyα break corresponding to $z = 11.09^{+0.08}_{-0.12}$ (ref. 2). However, its accurate redshift remained unclear. Here we report a probable detection of three ultraviolet (UV) emission lines from GN-z11, which can be interpreted as the [C III] λ1907, C III] λ1909 doublet and O III] λ1666 at $z = 10.957\pm0.001$ (when the Universe was only ~420 Myr old,

GN-z11 - кандидат на z ~ 11 – HST (WFC3) по положению Lyα break

Oesch, P. A. et al. A remarkably luminous galaxy at z = 11.1 measured with HST grism spectroscopy. *Ap. J.* **819**, 129-139 (2016).

- MUV = −22.1 ± 0.2, which is roughly a magnitude brighter than the characteristic luminosity of galaxies at z ~ 7–8.
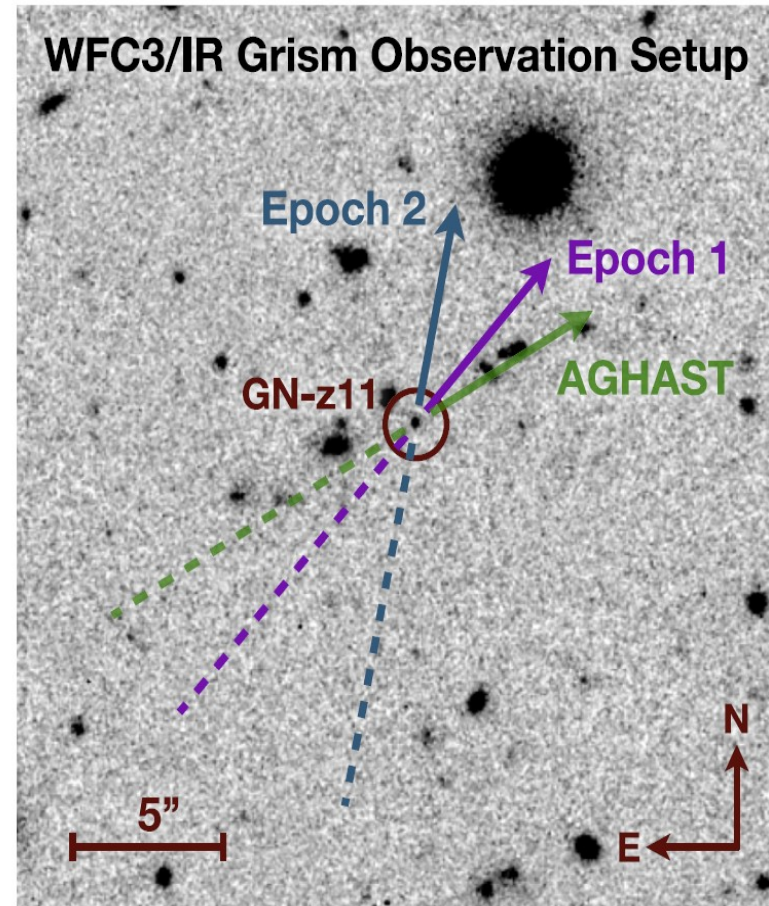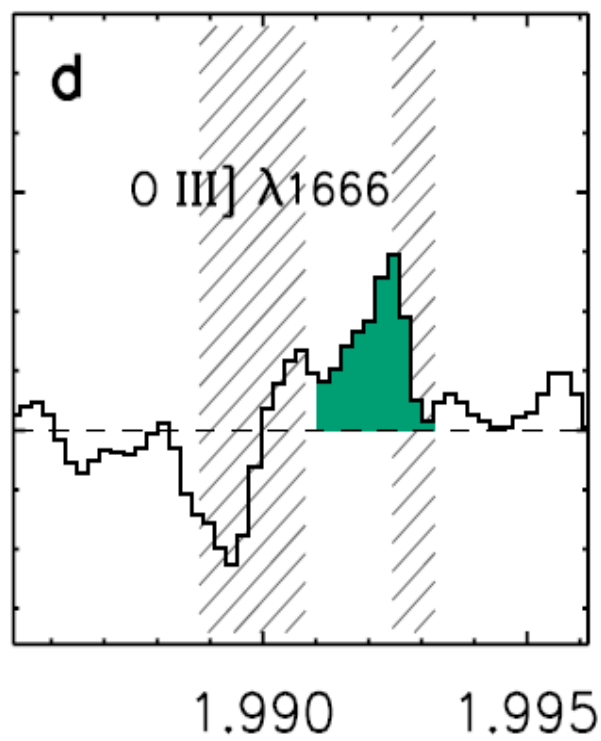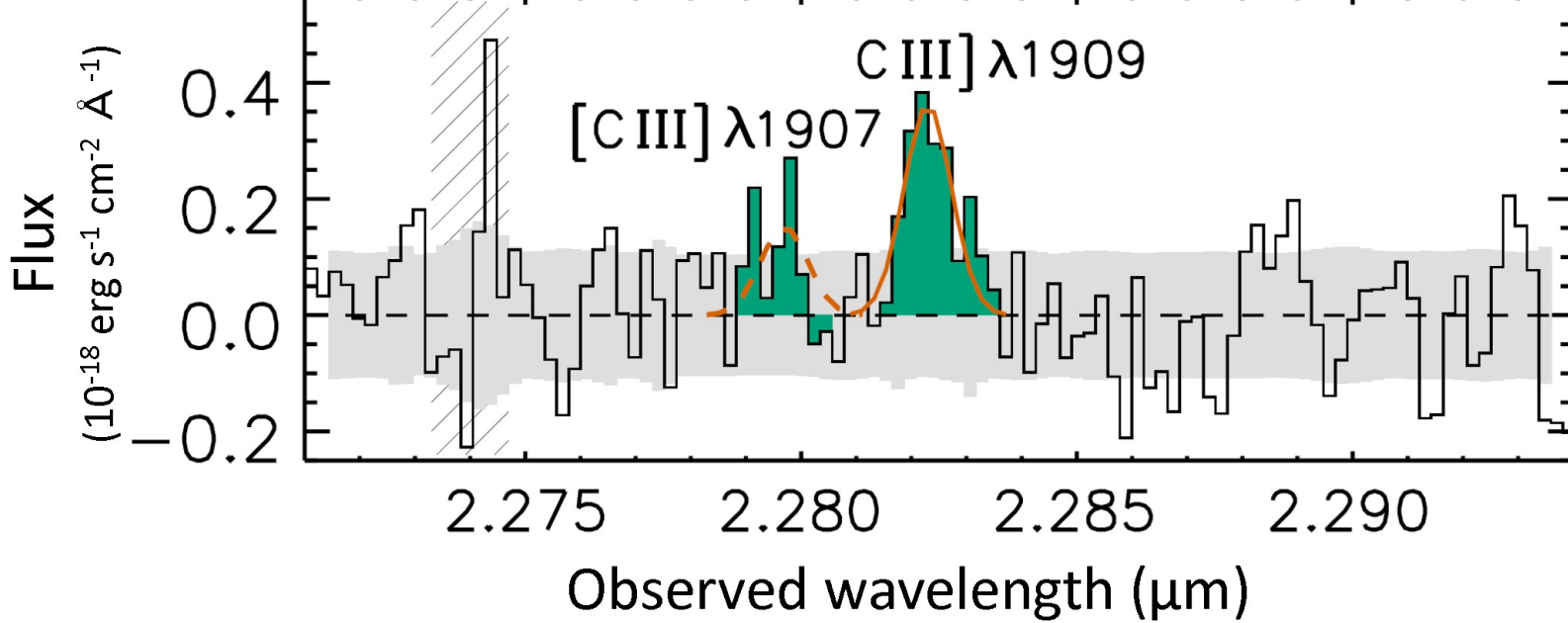

Figure 1. CANDELS *H*-band image around the location of our target source GN-z11. The arrows and dashed lines indicate the direction along which sources are dispersed in the slitless grism spectra for our two individual epochs (magenta and blue) and for the pre-existing AGHAST data (green). The latter are significantly contaminated by bright neighbors along the dispersion direction of GN-z11 (see Figure 2).

Keck I

- We search for line emission in the *K* band and identify a line at 19922 A and a line pair at 22797 and 22823 A, with significance of 3.3σ, 2.6σ, and 5.3σ, respectively. Taking the broadband photometry into consideration, we rule out the possibility that these lines are from a low-redshift galaxy.

[C III] λ1907

C III] λ1909

Flux
(10^{-18} erg s^{-1} cm^{-2} Å^{-1})

0.4

0.2

0.0

−0.2

2.275   2.280   2.285   2.290

Observed wavelength (μm)

d

O III] λ1666

1.990   1.995

Фотоионизационная модель: должен быть вклад AGN

Comparison with lower redshift galaxies having the

strongest C III] emission known in t

A single stellar population model (Model 1; bla

a binary stellar population model (Model 2; gr

Model 1 plus 10% contribution from an AGN (N

blue),

Model 3 plus an enhanced carbon abundance

(Model 4; orange),

and two AGN NLR models (Models 5 and 6; do

 dashed purple).
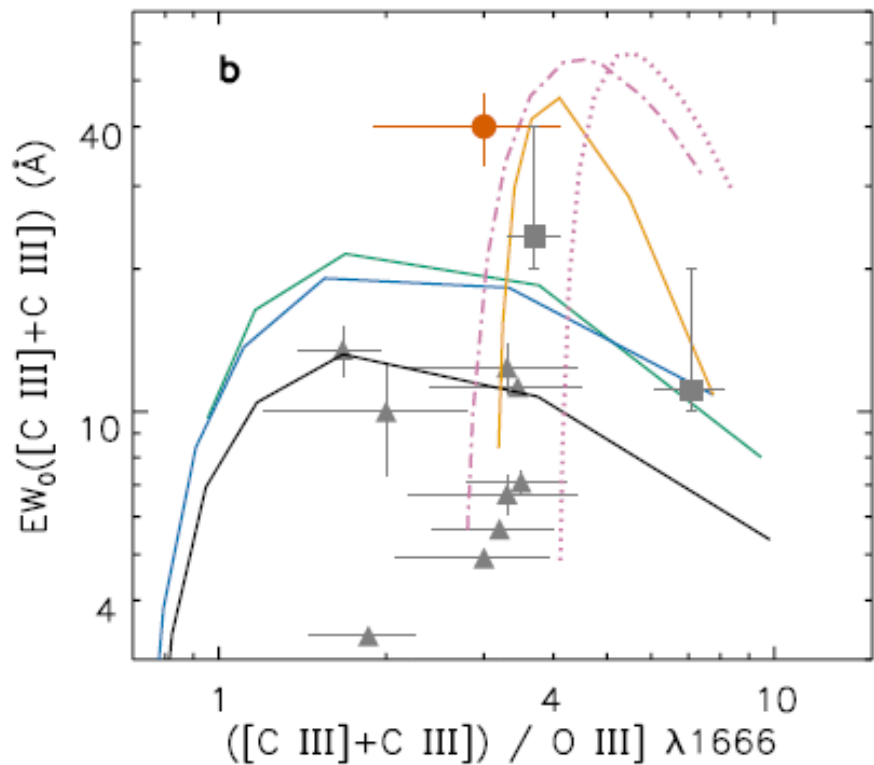
Сравнение с z = 3.558 и 5.124

Extended Data Fig. 4 SED modelling of GN-z11. (a): SED modelling result using a fixed redshift z = 3.558, i.e., the emission line at 22823 Å is assumed to be [O III] λ5007. The red points with 1σ error bars are the observed photometric data points. The downward arrows indicate the 2σ detection upper limits. The horizontal errors indicate the wavelength ranges of the filters. The light blue spectrum represents the best model. The dark blue crosses represent the photometric points predicted by the model. They are inconsistent with the observed values. For comparison, the grey spectrum represents the best model using a fixed redshift z = 10.957. The model photometry (black crosses) is well consistent with the observed photometry. (b): Same as (a), but for a fixed redshift z = 5.124, i.e., the emission line at 22823 Å is assumed to be [O II] λ3727. The best model is also inconsistent with the observed photometry.

Table 1. Properties of GN-z11
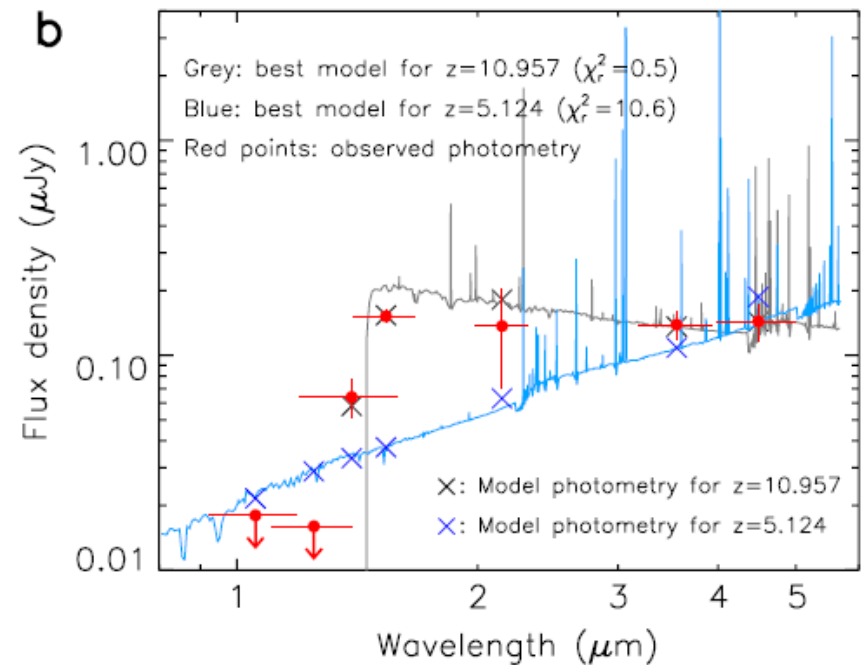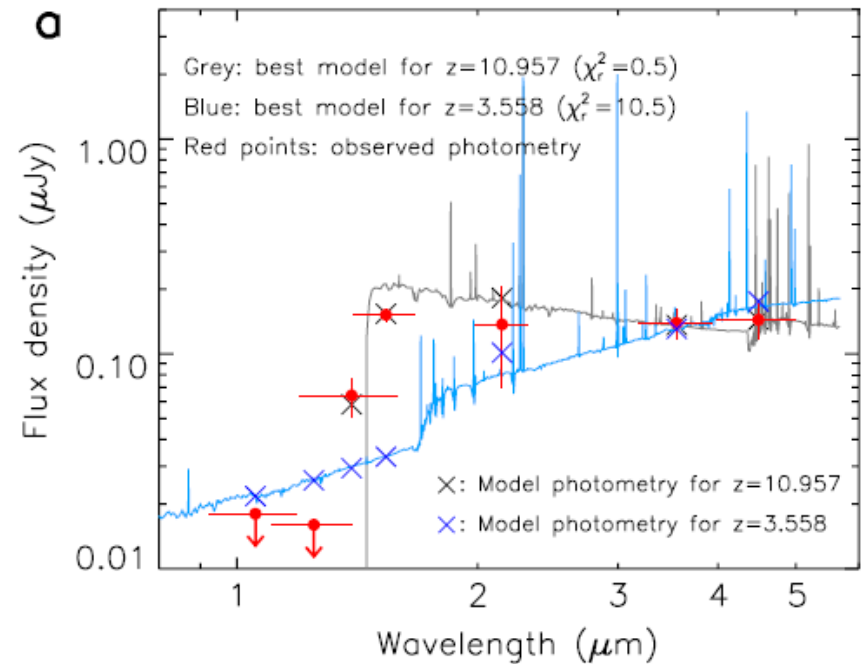
Parameters	Values
R.A. (hh:mm:ss)	12:36:25.46
Dec. (°:':")	+62:14:31.4
Redshift	10.957 ± 0.001
Flux ([C III] $\lambda1907$) (erg s^{-1} cm^{-2})	$(1.5 \pm 0.6) \times 10^{-18}$
EW$_0$ ([C III] $\lambda1907$) (Å)	12 ± 5
Flux (C III] $\lambda1909$) (erg s^{-1} cm^{-2})	$(3.5 \pm 0.7) \times 10^{-18}$
EW$_0$ (C III] $\lambda1909$) (Å)	28 ± 5
FWHM (C III] $\lambda1909$) (km s^{-1})	92 ± 23
Flux (O III] $\lambda1666$) (erg s^{-1} cm^{-2})	$(1.7 \pm 0.5) \times 10^{-18}$
EW$_0$ (O III] $\lambda1666$) (Å)	10 ± 3
UV continuum slope β	-2.4 ± 0.2
UV SFR ($M_\odot$ yr^{-1})	26 ± 3
Specific SFR (yr^{-1})	$(2.0 \pm 0.9) \times 10^{-8}$
Dust reddening $E(B-V)$ (mag)	0.01 ± 0.01
Age (Myr)	70 ± 40
Stellar mass ($M_\odot$)	$(1.3 \pm 0.6) \times 10^{9}$

A cuspy dark matter halo

Yong Shi,[1,2] Zhi-Yu Zhang,[1,2] Junzhi Wang,[3] Jianhang Chen,[1] Qiusheng Gu,[1,2] Xiaoling Yu,[1] and Songlin Li[1]

[1] *School of Astronomy and Space Science, Nanjing University, Nanjing 210093, China.*
[2] *Key Laboratory of Modern Astronomy and Astrophysics (Nanjing University), Ministry of Education, Nanjing 210093, China.*
[3] *Shanghai Astronomical Observatory, Chinese Academy of Sciences, 80 Nandan Road, Shanghai 200030, China*

ABSTRACT

The cusp-core problem is one of the main challenges of the cold dark matter paradigm on small scales: the density of a dark matter halo is predicted to rise rapidly toward the center as $\rho(r) \propto r^\alpha$ with α between -1 and -1.5, while such a cuspy profile has not been clearly observed. We have carried out the spatially-resolved mapping of gas dynamics toward a nearby ultra-diffuse galaxy (UDG), AGC 242019. The derived rotation curve of dark matter is well fitted by the cuspy profile as described by the Navarro-Frenk-White model, while the cored profiles including both the pseudo-isothermal and Burkert models are excluded. The halo has α= -(0.90±0.08) at the innermost radius of 0.67 kpc, $M_{\rm halo}$=(3.5±1.2)×10^{10} M$_\odot$ and a small concentration of 2.0±0.36. AGC 242019 challenges alternatives of cold dark matter by constraining the particle mass of fuzzy dark matter to be $< 0.11×10^{-22}$ eV or $> 3.3×10^{-22}$ eV, the cross section of self-interacting dark matter to be < 1.63 cm^2/g, and the particle mass of warm dark matter to be > 0.23 keV, all of which are in tension with other constraints. The modified Newtonian dynamics is also inconsistent with a shallow radial acceleration relationship of AGC 242019. For the feedback scenario that transforms a cusp to a core, AGC 242019 disagrees with the stellar-to-halo-mass-ratio dependent model, but agrees with the star-formation-threshold dependent model. As a UDG, AGC 242019 is in a dwarf-size halo with weak stellar feedback, late formation time, a normal baryonic spin and low star formation efficiency (SFR/gas).

1. INTRODUCTION

The cosmological model of cold dark matter and dark energy, i.e., ΛCDM, has achieved tremendous success in understanding the cosmic structure across time on large scales, but this model is challenged by observations on small scales such as the cusp-core problem, the missing dwarf problem, the too-big-to-fail problem etc. (for a review, see Weinberg et al. 2015).

In cosmological simulations of cold and collisionless

tral profiles in individual galaxies (Carignan & Beaulieu 1989; Lake et al. 1990; Jobin & Carignan 1990). Studies with higher spatial resolutions for a larger sample of dwarfs and low-surface-brightness galaxies further confirm the central flatness of the rotation curve, and derived a median dark-matter density slope of about -0.2 toward centers (de Blok et al. 2001; Oh et al. 2011, 2015). Optical observations of ionized gas such as Hα can achieve higher spatial resolutions than the HI data,

Too-big-to-fail problem etc. (for a review, see Weinberg et al. 2015).

- Optical observations of ionized gas such as H\alpha

can achieve higher spatial resolutions than the HI data, and confirmed the median density slope of about -0.2 with long-slit spectra for a large sample of dwarf galaxies.

- Among few galaxies whose halos can be described by cuspy proles, the one with the highest signal-to-noise ratio is DDO 101 and Draco.

- In order to identify a definitive cuspy dark matter halo, it is required to demonstrate not only the validity of cuspy models but also the invalidity of cored models.

- The orbital anisotropy, the method to model stellar orbits, the dark-matter shape and the limited number of the member stars are all found to affect the conclusions.

Открыт по обзору Arecibo в 2017
V_{corr} = 2237km/s

AGC
242019
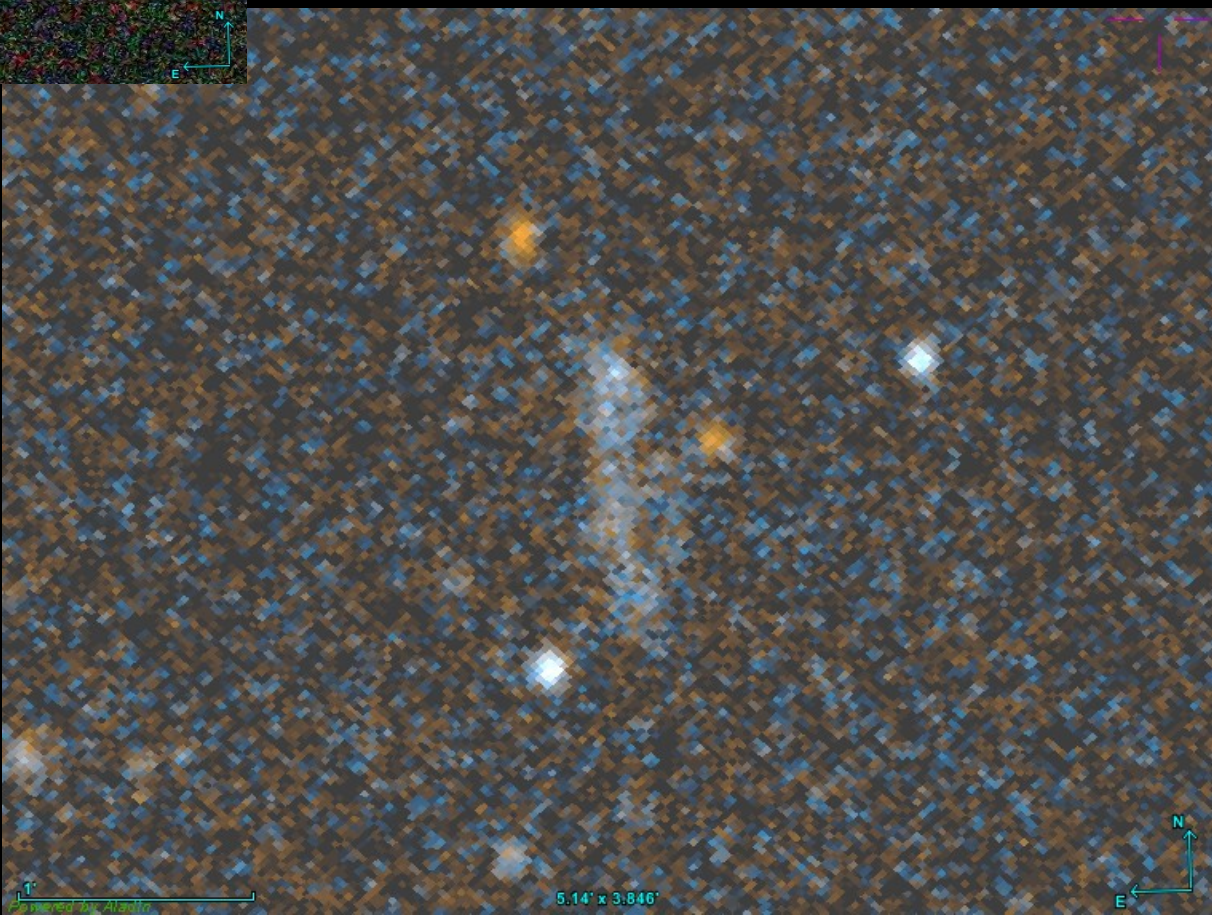
Parameters	Mean
M_{star} ($10^8 M_\odot$)	1.37
M_{HI} ($10^8 M_\odot$)	8.51
SFR ($10^{-3} M_\odot/yr$)	8.2
Dynamical center* (J2000)	14:33:53.38, 01:29:12.5
V_{sys}^* (km s^{-1})	1840.4
Distance (Mpc)	30.8
$\log(\Upsilon_{3.6\mu m}$ ($M_\odot/L_{\odot,3.6\mu m}$))	-0.22
R_{200} (NFW) (kpc)	65.0
R_S (NFW) (kpc)	33.3
concentration (NFW)	2.0
M_{halo} (NFW) ($10^{10} M_\odot$)	3.5
V_{norm} (ISO) (km s^{-1})	16.7
R_C (ISO) (kpc)	2.5

Любопытно: M_{star}/SFR = 1.6 10^{10} yr
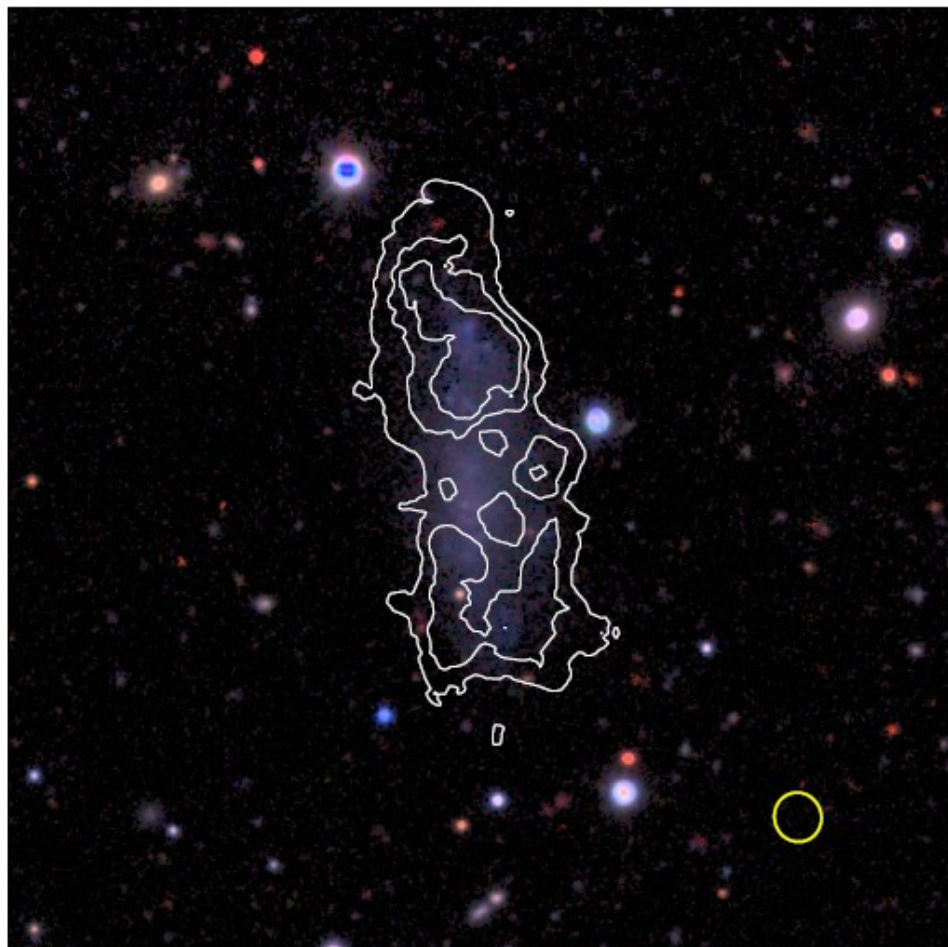
Figure 1. False-color image of AGC 242019. The false-color image of the g, r and z bands. The white contours of the HI intensity are at levels of 0.4, 0.6 and 0.8 mJy km s^{-1}. The yellow ellipse indicates the HI beam size.
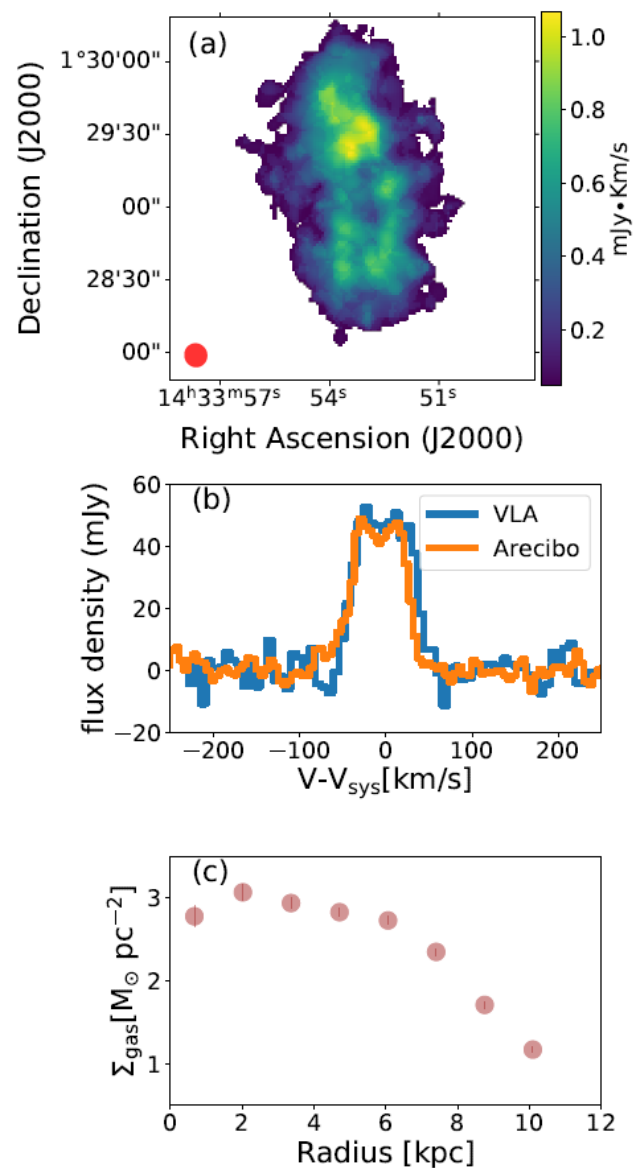

Figure 2. The HI data of AGC 242019. a, The HI intensity. b, The integrated spectra of the VLA compared to the Arecibo's spectrum (Haynes et al. 2018). c, The radial profile of the gas mass surface density corrected for inclination and helium.

НАБЛЮДЕНИЯ:

- HI VLA
- **3.6**&4.5 mkm WISE
- Обзор DECALS (g, r)
- WiFeS Australian NU 2.3м (Hα)
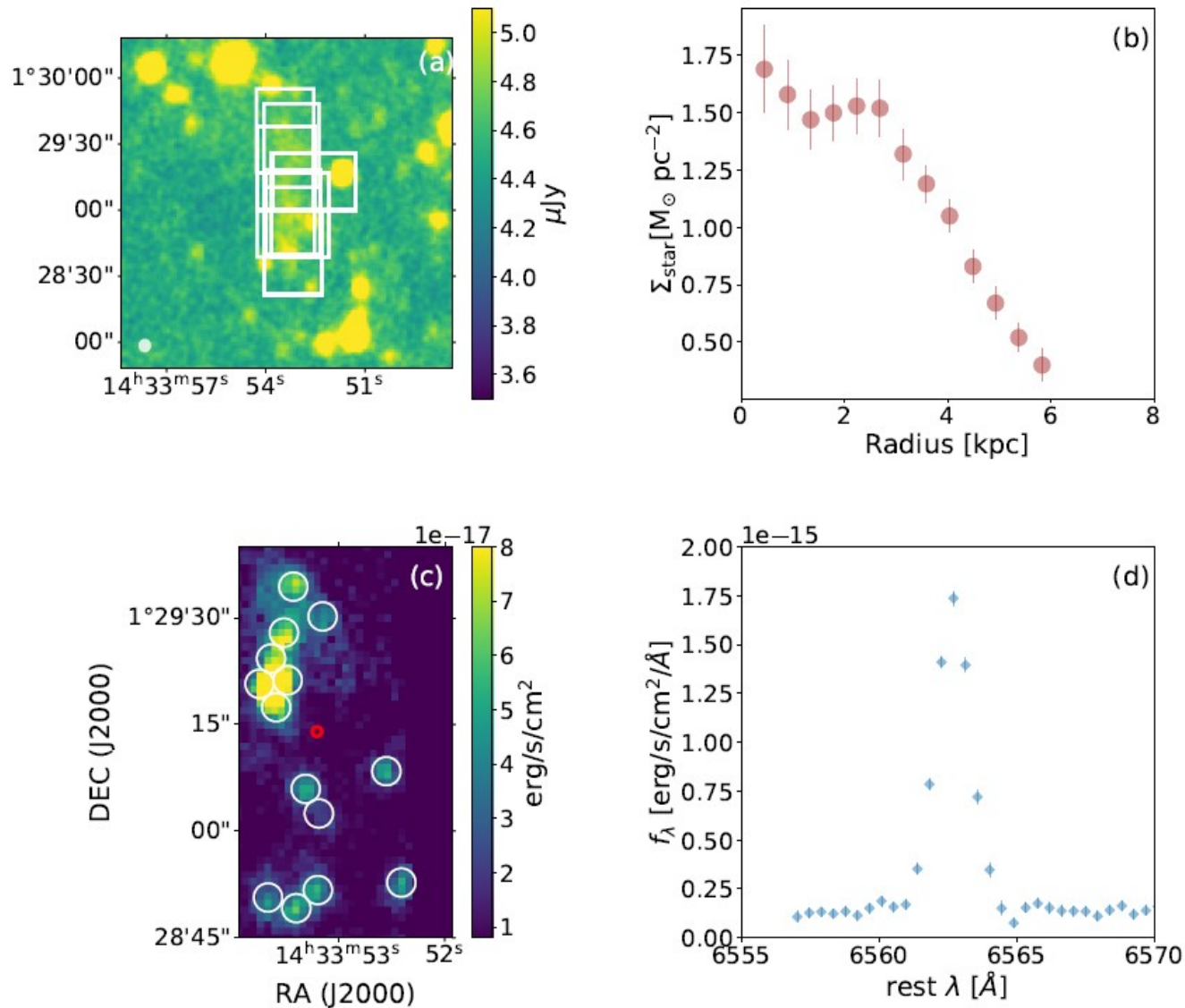
Figure 4. The infrared and optical data of AGC 242019. **a,** The 3.6 μm flux density with overlaid WiFeS IFU pointings. **b,** The radial profile of the stellar mass surface density corrected for the inclination. **c,** Individual Hα clumps for which the line of sight velocities are measured. Each clump has a circular radius of 2.0''. The small red circle indicates the dynamical center. **d,** The integrated spectrum of Hα emissions.
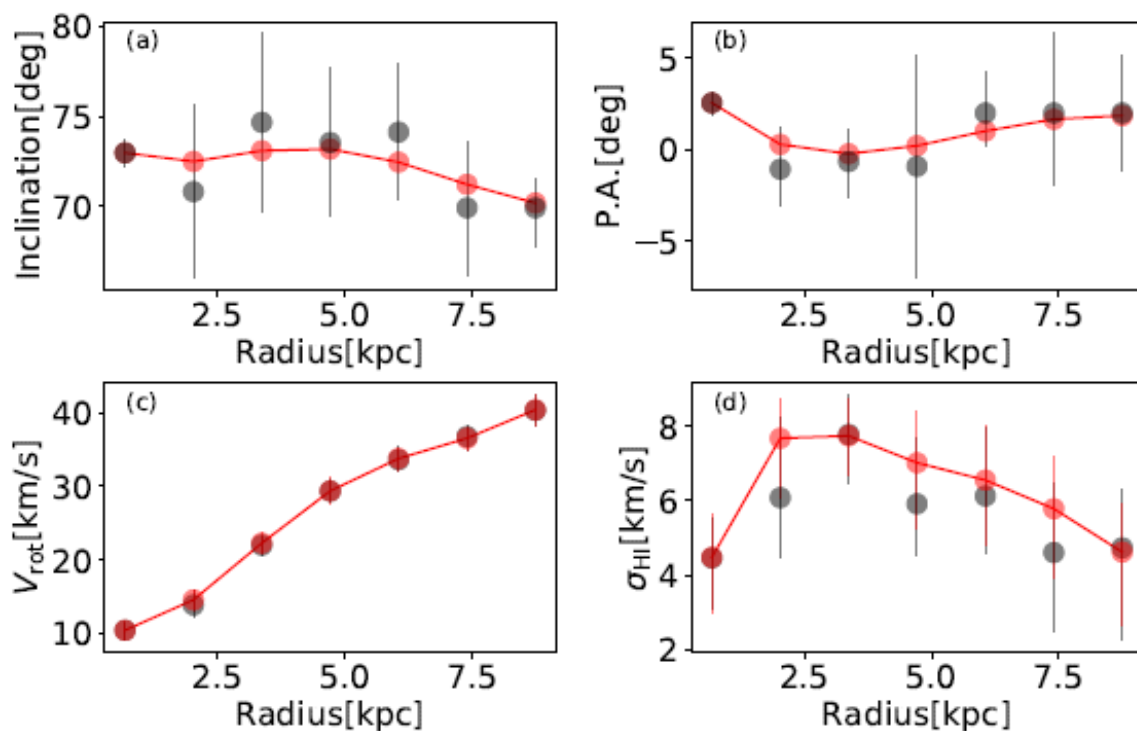
Figure 5. The two-stage operation of ^{3D}Barolo. The gray points are the first stage, where four parameters of each ring are set as free. The red points are the second stage, where the inclination and position angles are regularized by fitting a Bezier function to the results from the first stage.
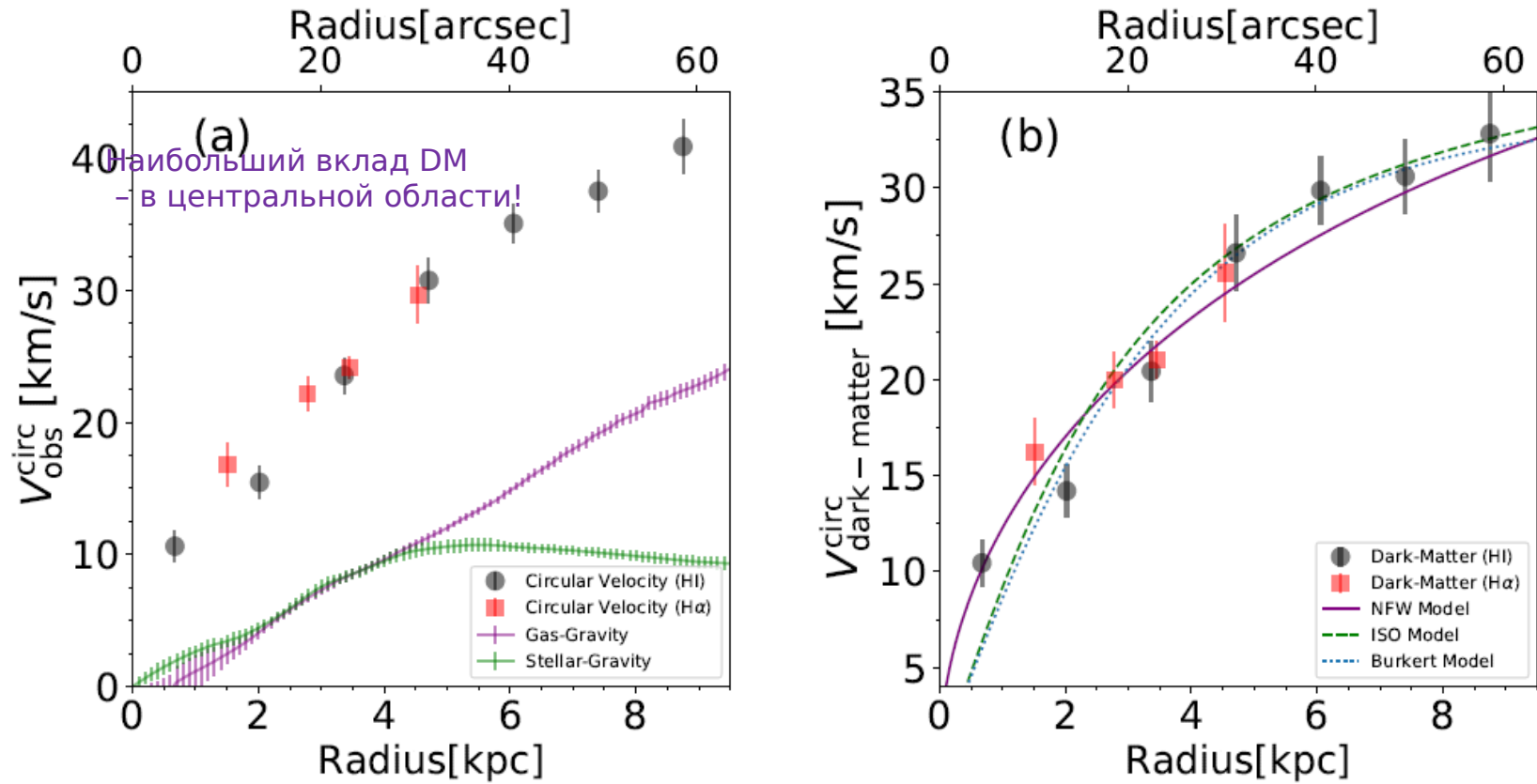
Figure 9.   The rotation curves of AGC 242019. **a,** The observed rotation curves from the HI data (black circles) and the Hα data (red rectangles), along with the rotation curves due to the gas and stellar gravity contributions. **b,** The derived rotation curve of dark matter. Different curves indicate the best-fitted NFW, ISO and Burkert models to the HI only rotation curve.
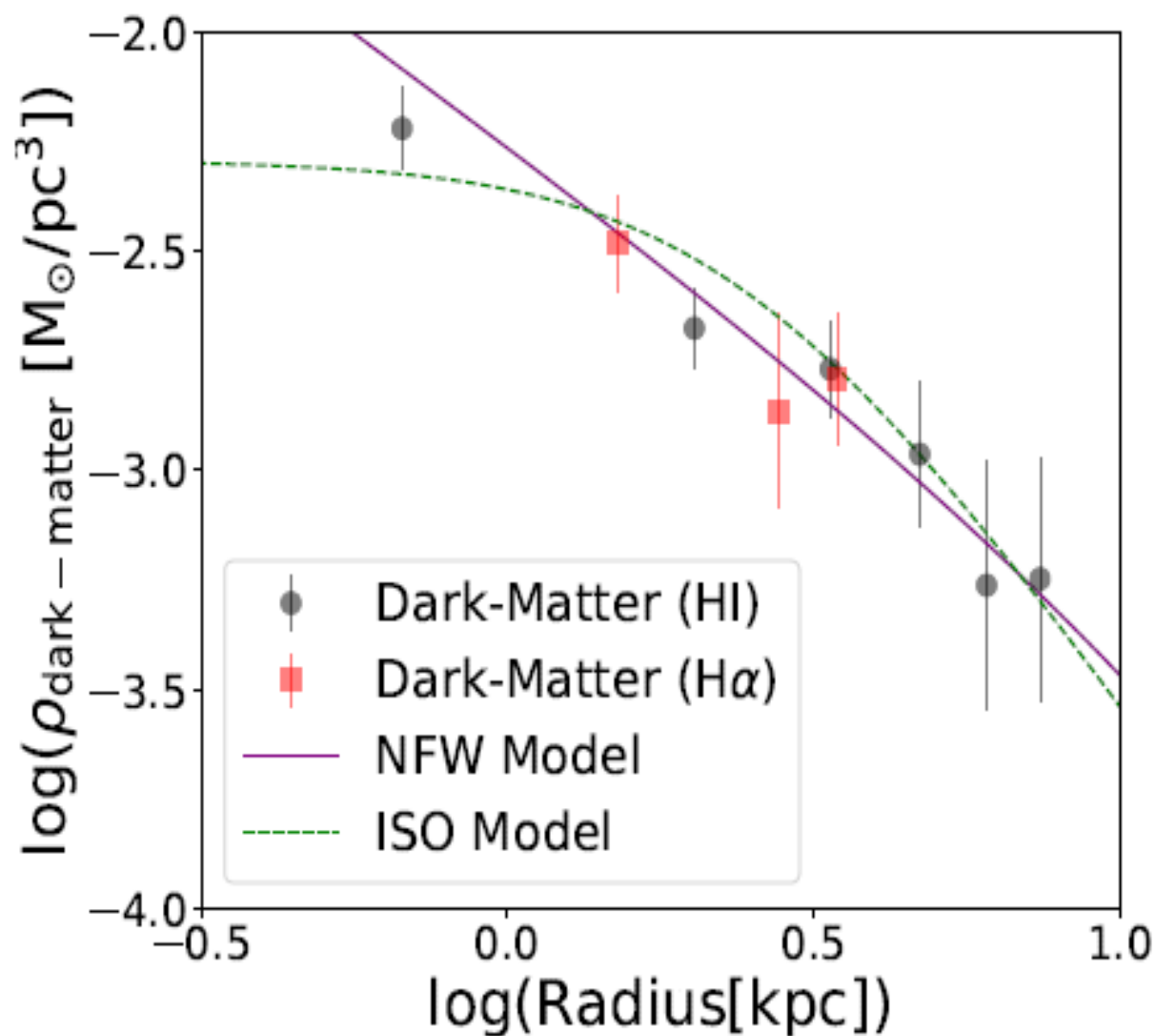
Figure 11. The density profile of dark matter of AGC 242019. Two curves represent the best-fitted NFW and ISO models to the HI rotation curve.
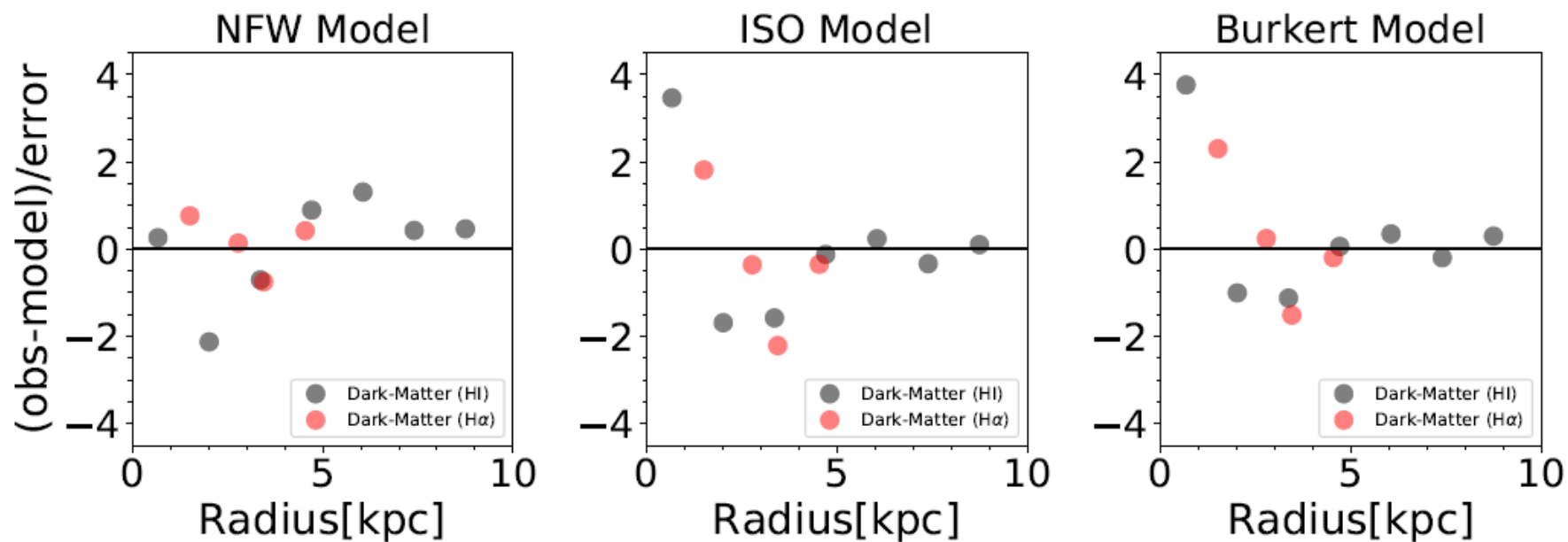
Figure 10. The residuals of the fitting to the dark-matter rotation curve for three models.

Оценены ограничения на параметры DM в сценариях, альтернативных cold DM

- Fuzzy cold DM

It is found that the measurements at the innermost two radii give the strongest constraints on m .

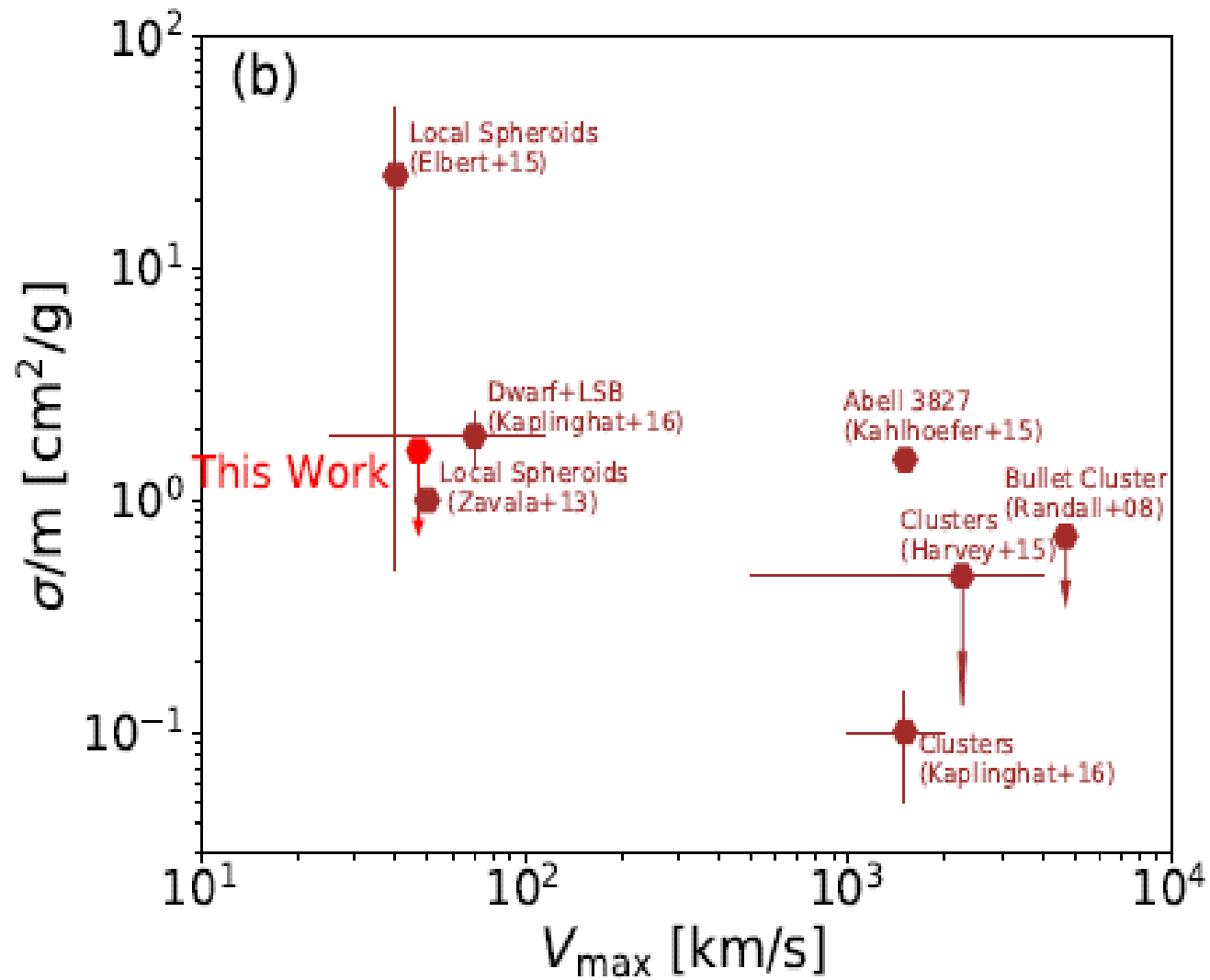- Рассеяние частиц DM (self-interacting DM)

$\rho(r)(\sigma/m)v_{rms}(r)t_{age} \sim 1;$

- Warm DM
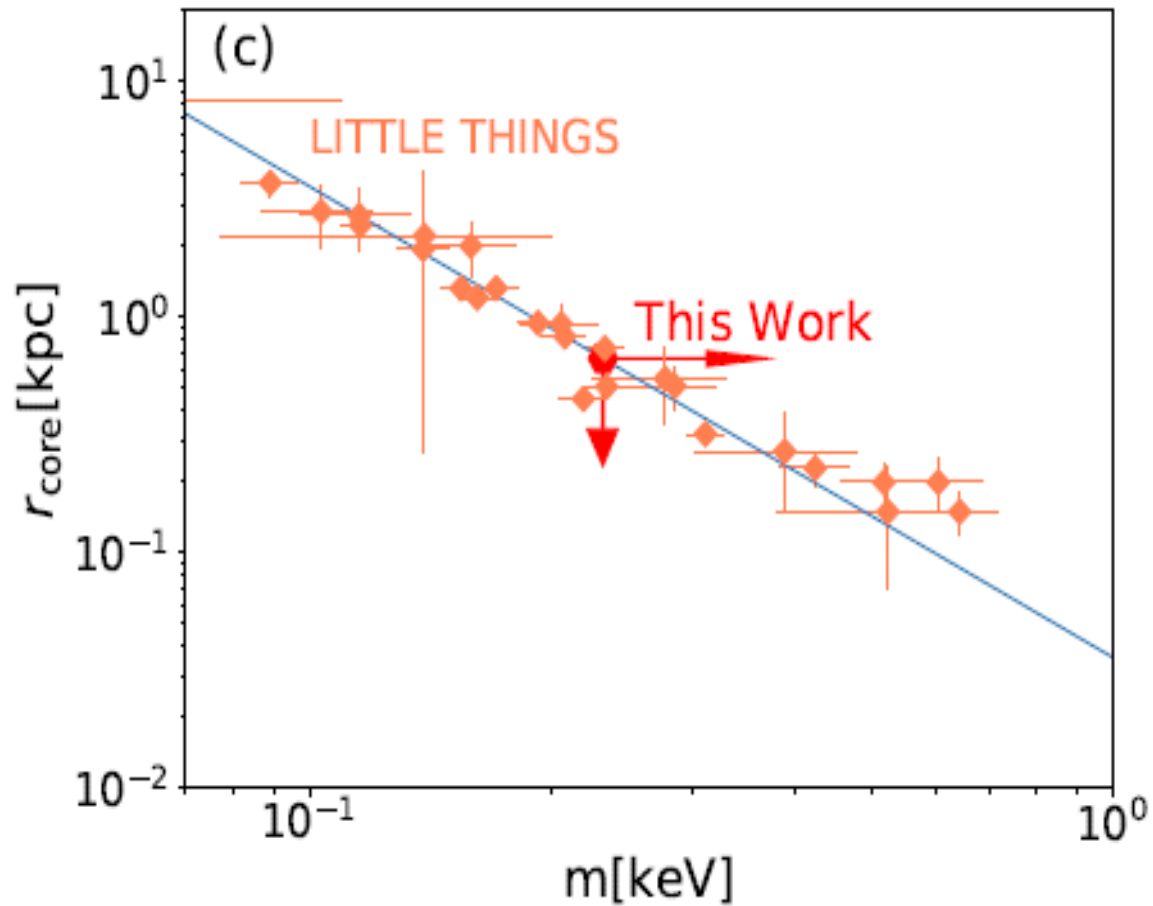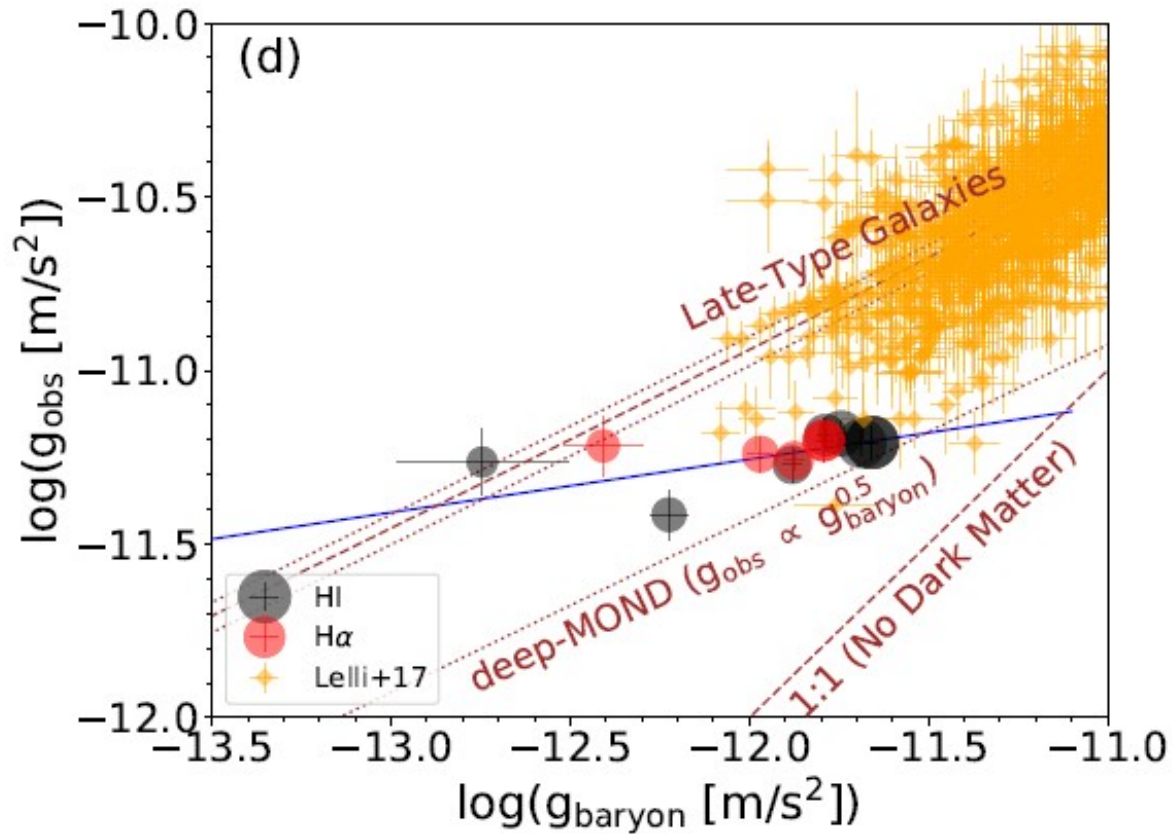
- MOND

- Stellar feedback (baryonic scattering)

(эффект зависит от M*/Mhalo,)

Ограничения на эфф.сечение рассеяния

Нижний предел масс частиц DM для «тёплой» DM

- The test of MOND through the relationship between the observed radial acceleration and the baryonic radial acceleration. The black/red symbols are the results of AGC 242019, where a larger symbol size corresponds to the ring with a larger radius. The blue solid line is the best linear fit to the observations.

- Lines labeled with \Late-Type Galaxies" and orange symbols are the best-tted line plus its scatter and individual late-type galaxies in Lelli et al. (2017). The dotted line labeled with \deep-MOND" is the MOND prediction in the low acceleration regime.

SFE соответствует низкой плотности барионной материи
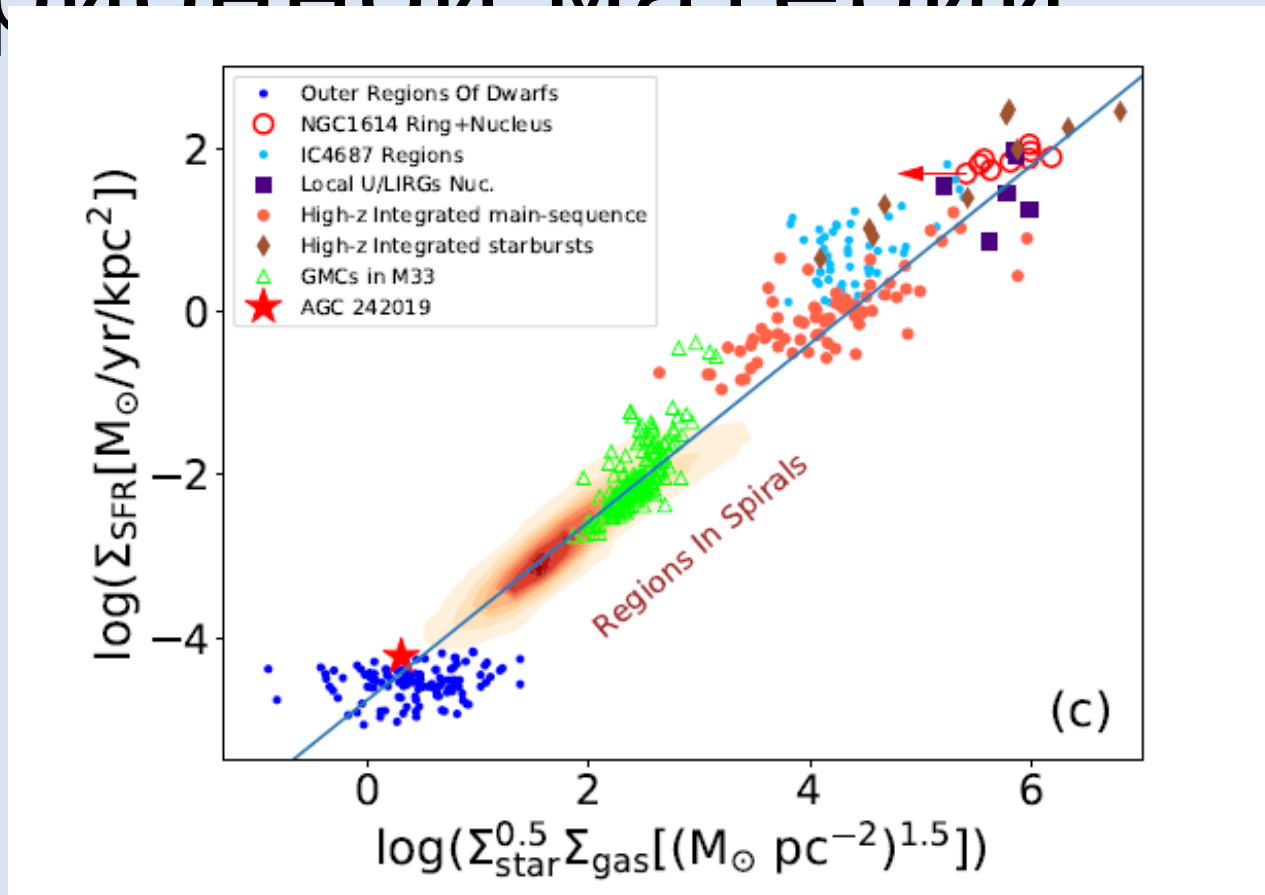
The location of AGC 242019 in the extended Schmidt law (Shi et al. 2018).

О природе объекта

- Раз есть касп, значит, не было сильного baryonic feedback в отличии от б-ва карликов.
- Гало имеет необычно низкую концентрацию.
- По удельному угл. моменту от обычных карликов не отличается (против модели формирования в гало с большим угл. моментом).
- Эффективность SF соответствует барионной плотности.
- По-видимому, галактика возникла из гало с низкой концентрацией плотности, и формирование ее должно быть более растянутым со временем. Касп – результат слабого feedback.
- Возможно, большая продолжительность SF является ключевым фактором, объясняющим низкую яркость галактики.